Original Research

Shortened derivatives from native antimicrobial peptide LyeTx I: *In vitro* and *in vivo* biological activity assessment

Leonardo Lima Fuscaldi[1],* ⓘ, **Joaquim Teixeira de Avelar Júnior[2],***,
Daniel Moreira dos Santos[2], **Daiane Boff[2]**, **Vívian Louise Soares de Oliveira[2]** ⓘ,
Karla Aparecida Guimarães Gusmão Gomes[3], **Rosana de Carvalho Cruz[4]**,
Patrícia Luciana de Oliveira[4], **Paula Prazeres Magalhães[4]**, **Patricia Silva Cisalpino[4]**,
Luiz de Macêdo Farias[4], **Elaine Maria de Souza-Fagundes[5]**, **Johannes Delp[6,7]** ⓘ,
Marcel Leist[6], **Jarbas Magalhães Resende[3]** ⓘ, **Flávio Almeida Amaral[2]** ⓘ,
Adriano Monteiro de Castro Pimenta[2], **Simone Odília Antunes Fernandes[1]**,
Valbert Nascimento Cardoso[1] and **Maria Elena de Lima[2,8]**

[1]Departamento de Análises Clínicas e Toxicológicas, Faculdade de Farmácia, Universidade Federal de Minas Gerais, Av. Antônio Carlos, 6627, Belo Horizonte, MG 31270-901, Brazil; [2]Departamento de Bioquímica e Imunologia, Instituto de Ciências Biológicas, Universidade Federal de Minas Gerais, Av. Antônio Carlos, 6627, Belo Horizonte, MG 31270-901, Brazil; [3]Departamento de Química, Instituto de Ciências Exatas, Universidade Federal de Minas Gerais, Av. Antônio Carlos, 6627, Belo Horizonte, MG 31270-901, Brazil; [4]Departamento de Microbiologia, Instituto de Ciências Biológicas, Universidade Federal de Minas Gerais, Av. Antônio Carlos, 6627, Belo Horizonte, MG 31270-901, Brazil; [5]Departamento de Fisiologia e Biofísica, Instituto de Ciências Biológicas, Universidade Federal de Minas Gerais, Av. Antônio Carlos, 6627, Belo Horizonte, MG 31270-901, Brazil; [6]*In Vitro* Toxicology and Biomedicine, University of Konstanz, Konstanz 78457, Germany; [7]Cooperative Doctorate College InViTe, University of Konstanz, Konstanz 78457, Germany; [8]Instituto de Ensino e Pesquisa, Santa Casa de Belo Horizonte, R. Domingos Vieira, 590, Belo Horizonte, MG 30150-242, Brazil
Corresponding author: Leonardo Lima Fuscaldi. Email: leonardo.fuscaldi@hotmail.com
*These authors contributed equally to this paper.

Impact statement

The resistance to antibiotics has been stressed by World Health Organization as one of the biggest threats to global health. So, new effective drugs against resistant microbes are imperative. In this research, we investigated three novel shortened peptides, derived from a natural antimicrobial peptide (LyeTx I) of spider venom, as potential antibiotics. This approach favors faster and cheaper synthesis, lower side effects and higher *in vivo* stability, by decreasing enzymatic degradation sites, which results in higher peptide bioavailability and impacts *in vivo* activity. Among the three shortened derivatives tested, LyeTx I mnΔK showed the best *in vitro* and *in vivo* antimicrobial activities. The *in vivo* activity was evaluated in a mouse model of septic arthritis, indicating the potential of this peptide as potent antibiotic agent. So, we suggest this peptide can be optimized to usage as antibiotic and advance the running for finding new antimicrobial agents.

Abstract

In the continuing search for novel antibiotics, antimicrobial peptides are promising molecules, due to different mechanisms of action compared to classic antibiotics and to their selectivity for interaction with microorganism cells rather than with mammalian cells. Previously, our research group has isolated the antimicrobial peptide LyeTx I from the venom of the spider *Lycosa erythrognatha*. Here, we proposed to synthesize three novel shortened derivatives from LyeTx I (LyeTx I mn; LyeTx I mnΔK; LyeTx I mnΔKAc) and to evaluate their toxicity and biological activity as potential antimicrobial agents. Peptides were synthetized by Fmoc strategy and circular dichroism analysis was performed, showing that the three novel shortened derivatives may present membranolytic activity, like the original LyeTx I, once they folded as an alpha helix in 2.2.2-trifluorethanol and sodium dodecyl sulfate. *In vitro* assays revealed that the shortened derivative LyeTx I mnΔK presents the best score between antimicrobial ($\downarrow$ MIC) and hemolytic ($\uparrow$ EC$_{50}$) activities among the synthetized shortened derivatives, and LUHMES cell-based NeuriTox test showed that it is less neurotoxic than the original LyeTx I (EC$_{50}$ [LyeTx I mnΔK] $\ggg$ EC$_{50}$ [LyeTx I]). *In vivo* data, obtained in a mouse model of septic arthritis induced by *Staphylococcus aureus*, showed that LyeTx I mnΔK is able to reduce infection, as demonstrated by bacterial recovery assay ($\sim$10-fold reduction) and scintigraphic imaging (less technetium-99m labeled-Ceftizoxime uptake by infectious site). Infection reduction led to inflammatory process and pain decreases, as shown by immune cells recruitment reduction and threshold nociception increment, when compared to positive control group. Therefore, among the three shortened peptide derivatives, LyeTx I mnΔK is the best candidate as antimicrobial agent, due to its smaller amino acid sequence and toxicity, and its greater biological activity.

Introduction

Antibiotic resistance and opportunistic infections have stimulated the search for new antimicrobial agents. In this sense, antimicrobial peptides (AMPs) are promising molecules, exhibiting different mechanisms of action from classic antibiotics. AMPs modulate host immunity or directly kill bacteria either by membrane disruption or by interaction with intracellular targets.[1–3] Although bacterial resistance to AMPs was initially considered as unlikely, different types of resistance are possible, like: (a) constitutive—when the bacterium possesses inherent properties that confer resistance to AMPs, even in the absence of bacterial exposure to AMPs; (b) inducible—when the bacterium activates genes that substitute, modify, or acylate membrane lipids to avoid their interactions with AMPs; and (c) acquired—by horizontal transfer of genes between bacteria.[4,5]

The AMPs are positively charged molecules and selectively interact with microorganism cells rather than with mammalian cells, due to negatively charged phospholipids at the outer leaflet of microorganism cytoplasmic membrane. Thus, they bind to microorganisms due to electrostatic and hydrophobic interactions. On the other hand, bindings between AMPs and mammalian cells own only to hydrophobic interactions, once their cytoplasmic membrane presents neutral outer leaflet.[6,7]

Previously, our research group isolated LyeTx I, a cationic peptide consisting of 25 amino acid residues, from the venom of *Lycosa erythrognatha*, known as wolf spider. This native peptide presents promising antimicrobial activity against bacteria and fungi, probably due to a membranolytic mechanism of action.[8] Beyond that, LyeTx I alone and 1:1 LyeTx I/β-cyclodextrin inclusion compound are effective against periodontal pathogens with rapid bactericidal effect and capable to reduce metabolic activity of planktonic and 2-day multispecies biofilm cells at concentrations $<250\,\mu g\cdot mL^{-1}$.[9,10] Further studies suggested that LyeTx I amino-terminal side is indispensable to the secondary structure conformation of the peptide, influencing its interaction with bacteria, once either the modification of LyeTx I carboxyl-terminal side (LyeTx I-K-HYNIC) or the suppression of a histidine residue in the same portion (LyeTx I-b) does not compromise its antimicrobial activity.[11,12] Recently, LyeTx I-b was formulated with carboxymethylcellulose and showed activity against a strain of *Staphylococcus aureus* resistant to penicillin, erythromycin, and ampicillin, acting in planktonic condition and reducing biofilm viability in 90%. Furthermore, it is very effective in the treatment of keratitis, with no signs of ocular toxicity in an *in vivo* eye infection model induced by the same bacterium.[13]

In this sense, different strategies can improve the activity of AMPs, such as those previously mentioned, β-cyclodextrin/carboxymethylcellulose formulation or amino acid residues sequence reduction. The latter favors faster and cheaper chemical synthesis, and possibly side effects reduction and *in vivo* stability increment, optimizing their usage as antibiotics.[14–16]

Therefore, the present work aimed to synthesize novel shortened derivatives from the native AMP LyeTx I, and to evaluate their toxicity and biological activity by *in vitro* assays and *in vivo* experimental model of septic arthritis.

Materials and methods

Materials

Amino acid derivatives were purchased from Iris Biotech GmbH (Marktredwitz, Germany). NaCl, KCl, trifluoroacetic acid (TFA) and triisopropylsilane were obtained from Sigma-Aldrich (Saint Louis, USA). Na_2HPO_4 and KH_2PO_4 were purchased from F. Maia Indústria e Comércio Ltda (Cotia, Brazil). 1,3-diisopropylcarbodiimide was acquired from Fluka (Steinheim, Germany). 1-hydroxybenzotriazole was purchased from NovaBiochem-Merck (Darmstadt, Germany). N,N-dimethylformamide (DMF) and diisopropyl ether were obtained from Vetec (Duque de Caxias, Brazil). Acetonitrile (HPLC grade) was acquired from JT Baker (Center Valley, USA). If not mentioned otherwise analytical grade solvents were used. All solvents used in reversed phase-high performance liquid chromatography (RP-HPLC) system (HPLC grade) were purchased from Tedia (Rio de Janeiro, Brazil). Ultrapure water, obtained through MilliQ® system of Millipore (Darmstadt, Germany), was used throughout. Bacteria and fungi strains of reference, *Escherichia coli* (ATCC® 25922), *Pseudomonas aeruginosa* (ATCC® 27853), *Acinetobacter baumannii* (ATCC® 19606), *S. aureus* (ATCC® 33591 and ATCC® 6538), *Staphylococcus epidermidis* (ATCC® 12228), *Cryptococcus neoformans* (ATCC® 24067), *Cryptococcus gattii* (ATCC® 32608), and *Candida krusei* (ATCC® 20029), were acquired from American Type Culture Collection—ATCC (Manassas, USA). Rabbit erythrocytes were purchased from CasaLab (Belo Horizonte, Brazil). Technetium-99 metastable (^{99m}Tc) was obtained from a ^{99}Mo/^{99m}Tc generator supplied by the Nuclear Energy Research Institute—IPEN (São Paulo, Brazil). Other reagents and solvents for the radiolabelling procedure were acquired from Sigma-Aldrich (São Paulo, Brazil).

Synthesis and purification of peptides

The original LyeTx I (control) and three shortened derivatives from LyeTx I (Table 1) were synthesized and purified as previously reported.[17]

Syntheses were performed by stepwise solid-phase using the N-9-fluorenylmethyloxycarbonyl (Fmoc) strategy

Table 1. LyeTx I (control) and three novel shortened derivatives from LyeTx I, and their respective *in silico* physicochemical parameters.

Peptide	ε [M^{-1}cm^{-1}]	Mon.M [Da]	Amino acid residues sequence	Theoretical pI
LyeTx I	5500	2830.73	**H**-IWLTALKFLGKNLGKHLAKQQLAKL-**NH₂**	10.60
LyeTx I mn	5500	1700.03	**H**-IWLTALKFLGKNLGK-**NH₂**	10.30
LyeTx I mnΔK	5500	1828.13	**H**-IWLT**K**ALKFLGKNLGK-**NH₂**	10.48
LyeTx I mnΔKAc	5500	1871.13	**Ac**-IWLT**K**ALKFLGKNLGK-**NH₂**	10.48

LyeTx I is the original peptide.
LyeTx I mn is the shortened derivative from LyeTx I, minimized to 15 amino acid residues.
LyeTx I mnΔK is the shortened derivative from LyeTx I, minimized to 15 amino acid residues + Lys residue included.
LyeTx I mnΔKAc is the shortened derivative from LyeTx I, minimized to 15 amino acid residues and acetylated + Lys residue included.
ε: molar extinction coefficient at 280 nm; Mon.M: monoisotopic mass; pI: isoelectric point.

on a rink amide resin (substitution grade 0.68 mmol·g^{-1}). Side chain protecting groups were as follows: *t*-butyl for threonine, *t*-butyloxycarbonyl for lysine and tryptophan, (triphenyl)methyl for asparagine, glutamine and histidine. Couplings were performed with 1,3-diisopropylcarbodiimide/1-hydroxybenzotriazole in DMF for 60–180 min. Deprotections (15 min, twice) were conducted by piperidine:DMF (1:4 | v:v). Cleavage from the resin and final deprotection were performed with TFA:water:triisopropylsilane (95.0:2.5:2.5 | v:v) at room temperature during 90 min. Cold diisopropyl ether was used to precipitate the products and, then, the crude peptide complexes were extracted with water:acetonitrile (1:1 | v:v), followed by freeze-drying.

Crude products were purified by RP-HPLC (Shimadzu, Japan) on a C$_{18}$ column (Discovery® BIO Wide Pore C$_{18}$ column: 5 μm, 250.0 × 4.6 mm), equilibrated with 0.1% (v:v) TFA in water (eluent A) and eluted by a segmented gradient of 0.1% (v:v) TFA in acetonitrile (eluent B): 0–6 min, 0% B; 6–12 min, 0%–30% B; 12–50 min, 30%–50% B; 50–55 min, 50%–100% B; 55–61 min, 100% B (flow = 1.0 mL·min^{-1}; detection = 220 nm).

Collected fractions were assessed by matrix-assisted laser desorption ionization time of flight mass spectrometer (MALDI-ToF-MS) analysis on AutoFlex III (Bruker Daltonics®, Germany). Briefly, samples were spotted onto a sample plate (MTP 384 Anchorchip, Bruker Daltonics®, Germany), mixed with a saturated solution of α-cyano-4-hydroxycinnamic acid and allowed to dry at room temperature (dried-droplet method). The mass spectrometer spectra were acquired in the positive reflector mode with external calibration (Peptide Calibration Standard II, Bruker Daltonics®, Germany).

Circular dichroism spectroscopy analysis

Secondary structures of the three shortened derivatives from LyeTx I were investigated by circular dichroism (CD), using a Jasco-715 spectropolarimeter (reads 190–280 nm with 0.2 nm of range), to evaluate peptide conformation in different solutions: 2.2.2-trifluorethanol (TFE); sodium dodecyl sulfate (SDS); dodecylphosphocholine (DPC).

In vitro antimicrobial activity evaluation

Antimicrobial activity was evaluated *in vitro* by microdilution test according to Clinical and Laboratory Standards Institute, employing three gram-negative (*E. coli*; *P. aeruginosa*; *A. baumannii*) and two gram-positive (*S. aureus*; *S. epidermidis*) bacteria strains, and three fungi strains (*C. neoformans*; *C. gattii*; *C. krusei*). Readouts were carried by determination of minimum inhibitory concentration (MIC), i.e. minimum peptide concentration observed in plate without microorganism growth, post-incubation at 37 °C for 24 h. MIC was expressed as *median* (*n* = 3). Each replicate was performed with a different colony, in duplicate. Minimum bactericidal concentration (MBC) and minimum fungicidal concentration (MFC) were also determined.

In vitro erythrocyte toxicity evaluation

Erythrocytes hemolysis produced by original LyeTx I and the three shortened derivatives from LyeTx I was evaluated as previously described.[8] Briefly, peptides were serially diluted (base 2) and incubated with 1% rabbit erythrocytes in phosphate buffered saline (PBS), at 37°C for 1 h. Post-incubation, mixtures were centrifuged (300 × g/5 min) and supernatants were read at A$_{405}$. Positive control was a 1% (v/v) triton X-100 solution in PBS and negative control was non-treated 1% rabbit erythrocytes in PBS. Half maximal effective concentration (EC$_{50}$) was calculated for each peptide, as well as minimum hemolytic concentration (MHC), i.e. peptide concentration in which 1% of erythrocytes is lysed. Statistical analysis was performed between original LyeTx I and the three shortened derivatives from LyeTx I by Akaike information criterion test.

In vitro cytotoxicity on LUHMES cells evaluation

Cytotoxicity was investigated by assessing the neurotoxicity parameter of original LyeTx I and shortened derivative LyeTx I mnΔK, as recently described.[18] In brief, Lund Human Mesencephalic (LUHMES) cells were kept in proliferation medium (Adv DMEM/F12 containing 2 mM L-glutamine, 1× N2 supplement) enriched with 40 ng·mL^{-1} recombinant human basic fibroblast growth factor and cultured in 5% CO$_2$ at 37°C. Cell culture dishes and flasks were coated with 50 μg·mL^{-1} poly-L-ornithine and 1 μg·mL^{-1} fibronectin. Differentiation to post-mitotic neurons was performed by changing the medium to differentiation medium (Adv DMEM/F12 containing 2 mM L-glutamine, 1× N2 supplement, 1 mM dibutyryl 3,5-cyclic adenosine monophosphate, 1 μg·mL^{-1} tetracycline, and 2 ng·mL^{-1} recombinant human glial cell-derived neurotrophic factor). After 48 h of differentiation (day 2), cells

were detached with 0.05% Trypsin/EDTA and seeded into 96 well plates (35,000 cells/well). For the assessment of (developmental) neurotoxicity, these cells were treated with the peptides 1 h after seeding and then incubated for 24 h. To measure neurite stability (mature neurites), cells were allowed to grow neurites for 72 h after seeding (i.e. day 5 of differentiation) and subsequently treated with peptides for 24 h. Peptides were added in a concentration range of 0.09–100 μM with 1:4 dilution steps in dimethyl sulfoxide (DMSO) added to the medium. Final concentration of DMSO solvent was always 0.1% (v/v). Image acquisition was performed 22–26 h after starting peptides treatment.

Image acquisition and quantification of cytotoxicity on LUHMES cells

LUHMES cells were live-stained with Hoechst H-33342 (1.0 μg·mL^{-1}) and calcein-AM (1.0 μM) for image acquisition. The neurite area (NA) was calculated as the total calcein positive area corrected for the somatic area, i.e. the Hoechst-positive area, expanded by a surrounding ring of 3.2 μm representing the neuronal body. The images were used simultaneously to assess viability: double positive cells were counted as viable cells, while Hoechst-positive objects without calcein stain were counted as dead cells. Viability (V) was expressed as (viable cells/total cells) × 100%.[19]

Three independent experiments were performed and data were averaged for each test concentration. The EC$_{50}$ to reduce V and NA of LUHMES cells with neurites in development (day 2) or mature (day 5) were calculated using GraphPad Prism (version 8.0.2), as previously described.[18]

Experimental model of septic arthritis

Central Vivarium of Federal University of Minas Gerais (Belo Horizonte, Brazil) supplied male C57/BL6 mice (~7 weeks). Animals were kept under suitable conditions, with regulated light–dark cycle (12 h:12 h) and *ad libitum* access to chow and water. All animal experiments comply with the Guide for the Care and Use of Laboratory Animals, adopted by the Ethics Committee in Animal Experimentation of Federal University of Minas Gerais (CEUA/UFMG): protocol number 236/2014.

At day 0, animals were anesthetized with a mixture of ketamine (60 mg·kg^{-1}) and xylazine (4 mg·kg^{-1}). Under sterile conditions, the right posterior joint was depilated and septic arthritis was induced, as previously described.[20] Infected mice were intra-articular (IA) injected with 10 μL of a *S. aureus* (ATCC® 6538) suspension (8 × 10^7 CFU·mL^{-1}). Negative control group was IA inoculated with 10 μL of sterile PBS, instead of *S. aureus* suspension, and received no treatment.

At days 2, 4, and 6, infected mice were IA treated with the reference drug clindamycin (7.35 nmol/IA injection), original LyeTx I (0.08 nmol/IA injection), or shortened derivative LyeTx I mnΔK (0.08 or 0.16 nmol/IA injection). Positive control group received sterile saline, instead of treatment.

At day 7, i.e. at day 1 post-treatment, mice were subjected to some investigations, as follows.

Bacterial recovery assay. Mice were euthanized in a CO$_2$ camera and, under sterile conditions, right posterior articulations were harvested from animals and macerated with 500 μL of sterile PBS. Then, the homogenates (100 μL) were plated in blood agar and incubated at 37°C for 24 h. Results were expressed as colony forming units per joint cavity (CFU/joint), $n = 5$–6.

Scintigraphic imaging with ^{99m}Tc-Ceftizoxime. Radiolabeling of ceftizoxime (CFT) with ^{99m}Tc was performed according to Diniz *et al.*[21] An aliquot of ^{99m}Tc-CFT (7.4 MBq) was intravenously administered into each animal. At 2 h post-injection, mice were anesthetized with a mixture of ketamine (80 mg·kg^{-1}) and xylazine (15 mg·kg^{-1}) and placed (supine position) under an animal gamma camera (Nuclide^{TM} TH 22-Mediso, Hungary) employing a low-energy high-resolution collimator. Images were acquired using 256 × 256 × 16 pixels matrix size with a ±10% energy window set at 140 keV for 5 min.

For quantitative analysis of ^{99m}Tc-CFT uptake by infectious focus, scintigraphic images were assessed by target to non-target ratio determination ($n = 5$). The infected (right) and contralateral (left) joints were delimited, followed by radioactivity determination in each area. Target to non-target ratio was calculated as equation (1)

$$\text{Target to non} - \text{target ratio} = \frac{\text{counts}_{(\text{infected articulation / right joint})}}{\text{counts}_{(\text{contralateral articulation / left joint})}} \quad (1)$$

Total and differential counts of inflammatory cells. Total and differential counts of inflammatory cells were determined as previously described.[22] Briefly, the right posterior joint was washed and 10 μL of the joint lavage was diluted (3×) in Turk erythrocyte lysing solution. Total count of inflammatory cells was performed in Neubauer chamber ($n = 5$). A measured quantity of 50 μL of bovine serum albumin 3% in PBS were added to the remaining of the joint lavage, and the final solution was cytocentrifuged in order to prepare slides for differential count of inflammatory cells (neutrophils and mononuclear). The staining procedure was performed with panotic dye (Laborclin, Paraná), and the differential count was performed under an optical microscope (100× magnification). One hundred cells were counted and the amount of each inflammatory cell was estimated by simple rule of three based on total inflammatory cells count ($n = 5$).

This specific assay was also conducted with non-infected mice, at day 7, i.e. at day 1 post-treatment, as well as at 6 h post-treatment with one dose of shortened derivative LyeTx I mnΔK ($n = 5$).

Removal threshold hyperalgesia. The measurement of the removal threshold hyperalgesia was performed by

means of the increasing paw pressure assay (von Frey electronic method).[22] Briefly, a digital analgesymeter (*Insight, EFF-301*), which consists of a pressure transducer connected to a digital strength counter expressed in grams (g), was used with an accuracy of 0.1 g. For the contact of the pressure transducer with the paw of mice, a polypropylene tip (0.5 mm in diameter) was connected. Thus, a manual and linearly increasing pressure was applied under the plant area of the paw of animals until the removal was observed ($n = 4$).

Statistical analysis

Quantitative data were expressed as "mean ± SEM." Cytotoxicity to LUHMES cells was expressed as "mean ± SEM" comparing with control (DMSO, 0.1%). Means of two groups were compared using Student's *t*-test. Means of three or more groups were compared using analysis of variance, followed by Tukey test for multiple comparisons, two-to-two. *P values* < 0.05 were considered significantly. Data were analyzed using GraphPad Prism (version 8.0.2). Friedman statistic test were performed for bacteria and fungi sets antimicrobial assays.

Results

Synthesis, purification, and circular dichroism spectroscopy analysis of peptides

The original LyeTx I and three shortened derivatives from LyeTx I were synthesized (Table 1) and purified by RP-HPLC (Supplementary Figure S1). For each one, an aliquot of 5 mg was injected per run and synthesis yields were obtained after purification: LyeTx I (47%); LyeTx I mn (39%); LyeTx I mnΔK (29%); LyeTx I mnΔKAc (45%). MALDI-ToF-MS analysis detected pure products (Supplementary Figure S1).

The conformations of the three shortened derivatives from LyeTx I were assessed by CD spectroscopy analysis (Figure 1), which showed that they present a random structuring in water and fold as an alpha helix structuring in TFE. In SDS, these derivatives folded very well, especially LyeTx I mnΔK and LyeTx I mnΔKAc. Nonetheless, in DPC, LyeTx I mnΔK presented the poorest structuring.

In vitro antimicrobial activity, erythrocyte toxicity, and cytotoxicity on LUHMES cells evaluation

In vitro antimicrobial activity data are summarized in Tables 2 and 3. Friedman statistical tests, inside the same bacteria specie, were also performed (Supplementary Figure S2). Results showed that the shortened derivatives LyeTx I mnΔK and LyeTx I mnΔKAc present higher antimicrobial activities than the shortened derivative LyeTx I mn, which is represented by smaller MICs, MBCs, and MFCs for almost all bacteria and fungi strains evaluated. However, comparing these parameters between peptides, an antimicrobial activity reduction was observed to the three novel shortened derivatives compared to the original LyeTx I.
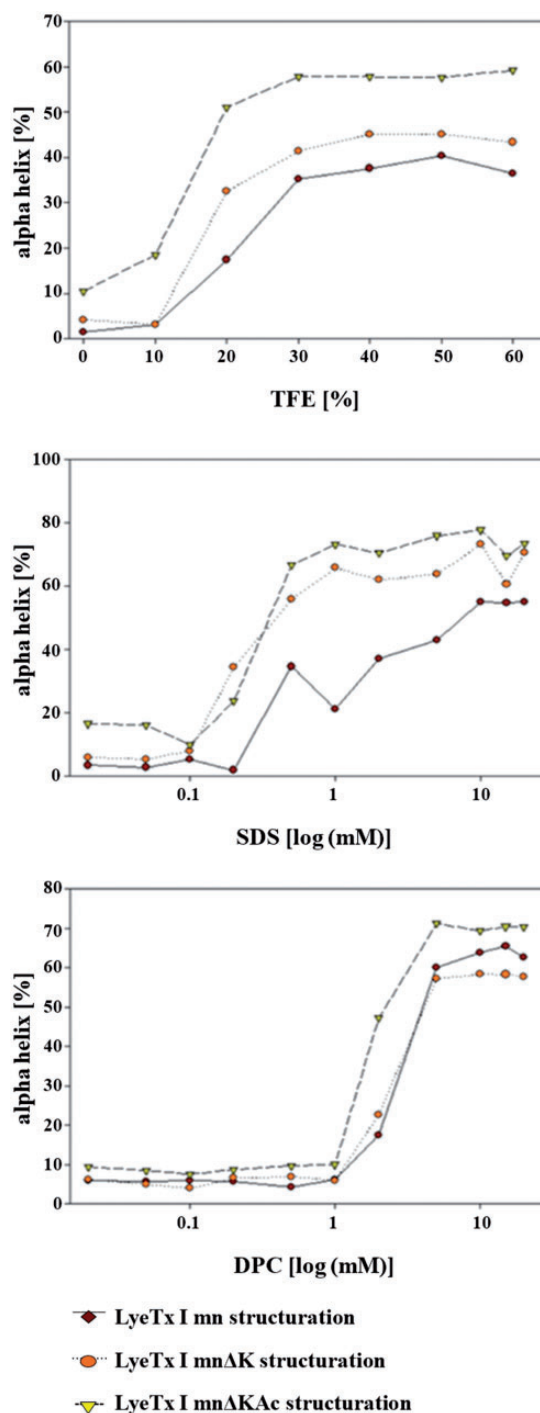

Figure 1. CD spectra deconvoluted by different TFE percentages, SDS and DPC concentrations. Data obtained after analysis in spectropolarimeter and deconvolution of them by CDPro software. (A color version of this figure is available in the online journal.)
DPC: dodecylphosphocholine; SDS: sodium dodecyl sulfate; TFE: 2.2.2-trifluorethanol.

In vitro erythrocyte toxicity data (Table 4; Figure 2) revealed lower hemolytic activities for the three novel shortened derivatives compared to the original LyeTx I, especially for LyeTx I mnΔK. Then, NeuriTox test was performed for this shortened derivative (LyeTx I mnΔK) and the original peptide (Figure 3). Similar EC_{50} values of V and NA were observed for each peptide after treatment of

Table 2. MIC values of the synthetic peptides, determined in bacteria and fungi strains.

Species	LyeTx I [µM]	LyeTx I [µg·mL⁻¹]	LyeTx I mn [µM]	LyeTx I mn [µg·mL⁻¹]	LyeTx I mnΔK [µM]	LyeTx I mnΔK [µg·mL⁻¹]	LyeTx I mnΔKAc [µM]	LyeTx I mnΔKAc [µg·mL⁻¹]	Reference drug [µM]	Reference drug [µg·mL⁻¹]
Escherichia coli (ATCC® 25922)	1.41	4.0	14.93	25.3	0.96	1.7	3.01	5.6	0.90*	0.2*
Pseudomonas aeruginosa (ATCC® 27853)	2.82	8.0	37.64	64.0	9.82	17.9	24.18	45.0	14.06*	15.6*
Acinetobacter baumannii (ATCC® 19606)	0.70	2.0	5.27	8.9	1.09	2.0	2.68	5.0	ND	ND
Staphylococcus aureus (ATCC® 33591)	0.70	2.0	4.70	8.0	3.08	5.6	4.27	8.0	99.03**	32.0**
Staphylococcus epidermidis (ATCC® 12228)	0.70	2.0	4.18	7.1	2.18	4.0	2.13	4.0	24.15**	7.8**
Cryptococcus neoformans (ATCC® 24067)	7.11	20.1	14.93	25.3	4.90	8.9	8.55	16.0	3.26***	0.9***
Cryptococcus gattii (ATCC® 32608)	2.23	6.3	3.73	6.3	1.73	3.1	3.38	6.3	52.25***	16.0***
Candida krusei (ATCC® 20029)	14.23	40.3	37.64	64.0	17.50	32.0	30.46	57.0	52.25***	16.0***

Reference drug: *tetracycline; **chloramphenicol; ***fluconazole.
ND: no data.

Table 3. MBC and MFC values of the synthetic peptides, determined in bacteria and fungi strains.

Species	LyeTx I [µM]	LyeTx I [µg·mL⁻¹]	LyeTx I mn [µM]	LyeTx I mn [µg·mL⁻¹]	LyeTx I mnΔK [µM]	LyeTx I mnΔK [µg·mL⁻¹]	LyeTx I mnΔKAc [µM]	LyeTx I mnΔKAc [µg·mL⁻¹]
Escherichia coli (ATCC® 25922)	2.82	8.0	14.93	25.3	2.17	4.0	8.55	16.0
Pseudomonas aeruginosa (ATCC® 27853)	2.82	8.0	37.64	64.0	11.02	20.1	34.20	64.0
Acinetobacter baumannii (ATCC® 19606)	1.41	4.0	5.92	10.0	1.09	2.0	4.27	8.0
Staphylococcus aureus (ATCC® 33591)	2.82	8.0	9.41	16.0	4.36	8.0	17.10	32.0
Staphylococcus epidermidis (ATCC® 12228)	0.70	2.0	4.70	8.0	2.18	4.0	2.13	4.0
Cryptococcus neoformans (ATCC® 24067)	7.96	22.6	31.36	53.3	7.29	13.3	14.25	26.6
Cryptococcus gattii (ATCC® 32608)	2.82	8.0	7.05	13.3	3.64	6.6	7.12	13.3
Candida krusei (ATCC® 20029)	22.60	64.0	37.64	128.0	35.00	64.0	68.40	128.0

Table 4. Erythrocytes toxicity of the synthetic peptides.

Peptide	EC₅₀ [µM]	MHC [µM]	EC₅₀ (statistical significance in function of LyeTx I)
LyeTx I	32.35	5.06	—
LyeTx I mn	381.40	48.06	>99.9% | $p < 0.01$
LyeTx I mnΔK	506.50	44.67	>99.9% | $p < 0.01$
LyeTx I mnΔKAc	207.50	27.44	>99.9% | $p < 0.01$

EC₅₀, MHC, and statistical significance of the original LyeTx I and the three novel shortened derivatives from LyeTx I.
EC₅₀: half maximal effective concentration to hemolysis; MHC: minimum hemolytic concentration.
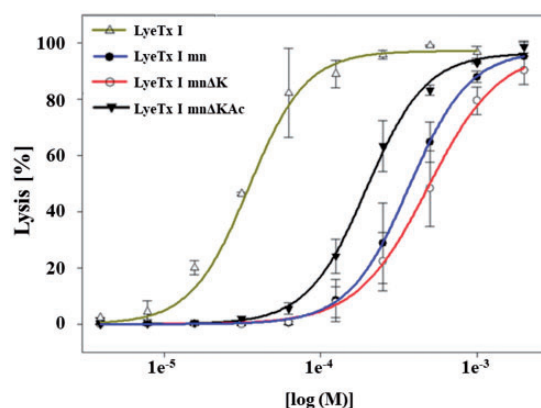

Figure 2. Hemolytic activities of synthetic peptides. Peptides were serially diluted (base 2) from 2.0 mM to 3.9 µM (except to original LyeTx I, which was incubated with 1 mM maximum) and incubated against 1% rabbit erythrocytes in PBS. EC₅₀ values and statistics are expressed in Table 4. (A color version of this figure is available in the online journal.)
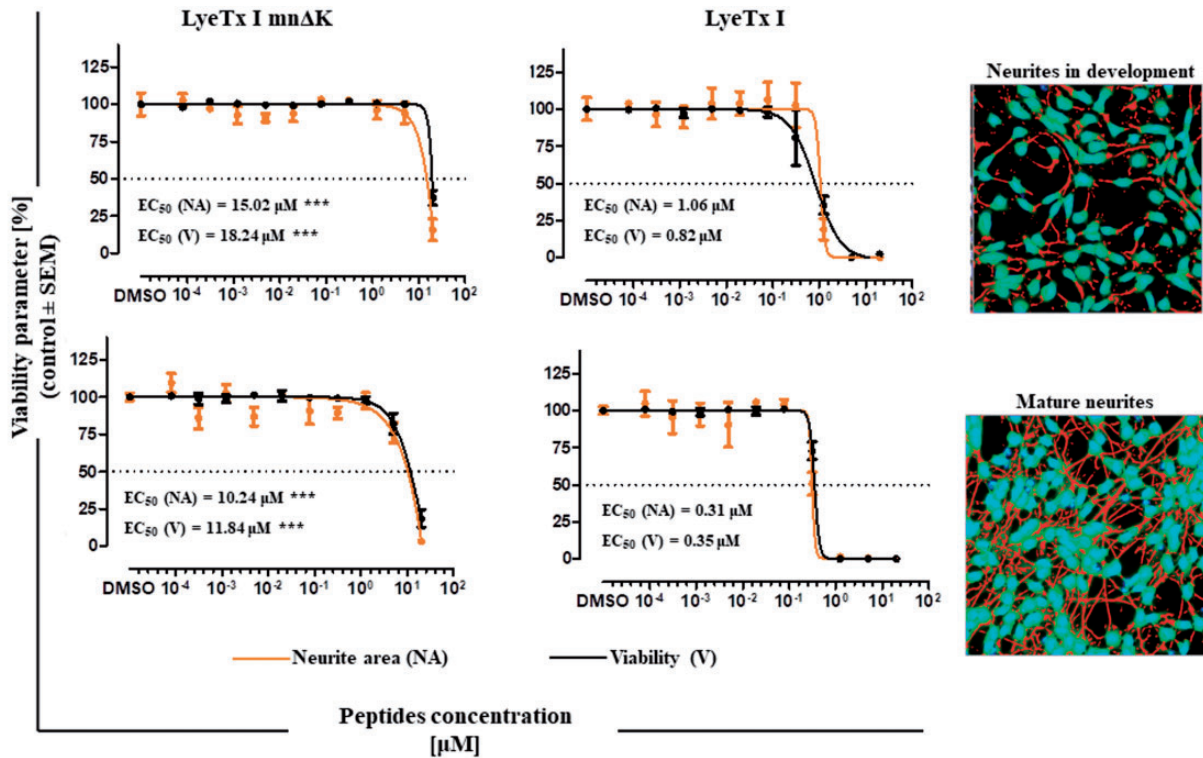
Figure 3. Cytotoxic effect of shortened derivative LyeTx I mnΔK and original LyeTx I on neurite area (NA) and viability (V) of LUHMES cells in different stages of neurite differentiation using the NeuriTox assay. LUHMES cells with neurites in development or mature neurites were treated with the peptides for 24 h. NA and V were evaluated using high content imaging (representative images on the right). EC_{50} values of NA and V were calculated using GraphPad Prism (version 8.0.2). The respective means between LyeTx I mnΔK and LyeTx I were compared using the Student's *t*-test (***$p < 0.001$). Representative data of "mean ± SEM" of three independent experiments in triplicate. (A color version of this figure is available in the online journal.)
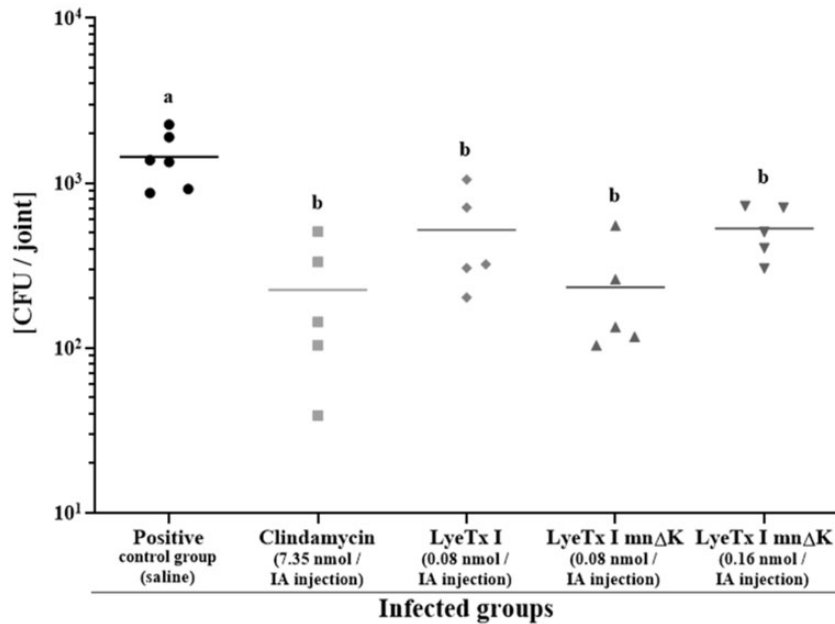
Figure 4. Bacterial recovery assay. Values are expressed as "mean" ($n = 5$–6). Means were compared using ANOVA, followed by Tukey test for multiple comparisons, two-to-two. Different letters indicate significant differences ($p < 0.05$).
CFU/joint: colony forming units per joint cavity.
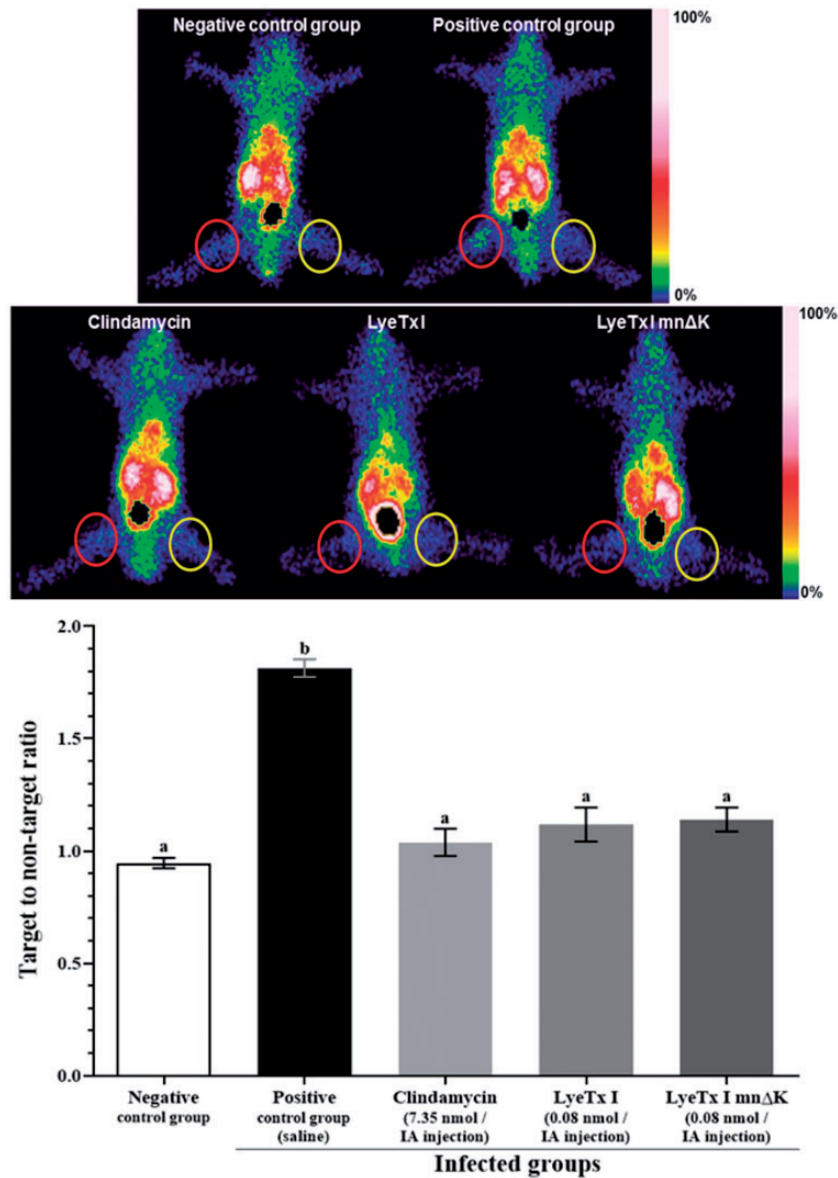
Figure 5. Scintigraphic images (256 × 256 × 16 matrix size) obtained at 2 h after intravenous injection of ^{99m}Tc-CFT (7.4 MBq) into mice ($n = 5$). Red circles indicate infectious foci and the corresponding area in negative control group mice. Yellow circles indicate the contralateral area. Target to non-target ratio was obtained by scintigraphic images quantitative analysis. Values are expressed as "mean ± SEM." Means were compared using ANOVA, followed by Tukey test for multiple comparisons, two-to-two. Different letters indicate significant differences ($p < 0.05$). (A color version of this figure is available in the online journal.)

LUHMES cells at different stages of differentiation. However, treatment of LUHMES cells with neurites in development with both peptides demonstrated that the EC$_{50}$ values obtained for the shortened derivative LyeTx I mnΔK for V and NA were, respectively, 22- and 14-fold higher than those obtained for original peptide. Furthermore, comparisons between both peptides showed a 33-fold increment in the EC$_{50}$ values (V and NA) for LyeTx I mnΔK, demonstrating its lower cytotoxicity.

In vivo assays in an experimental model of septic arthritis

To assess *in vivo* antimicrobial activity, bacterial recovery assay (Figure 4) and scintigraphic imaging using ^{99m}Tc-CFT (Figure 5) were performed. Bacterial recovery was

about 10-times lower for those treated infected groups compared to positive control group. Scintigraphic imaging revealed that ^{99m}Tc-CFT uptake was similar between right (sterile PBS inoculation) and left (contralateral area) posterior joint for negative control group, which was corroborated by target to non-target ratio of ~1.0. On the other hand, positive control group showed high ^{99m}Tc-CFT uptake by the infected joint, in accordance with target to non-target ratio of ~1.8. However, all treated infected groups exhibited similar ^{99m}Tc-CFT uptake by both joints, with no significant difference between them and negative control group.

The inflammatory process reduction was assessed by total and differential counts of inflammatory cells (Figure 6). No inflammatory cells recruitment was observed for negative control group (Figure 6(a)). On the other hand,
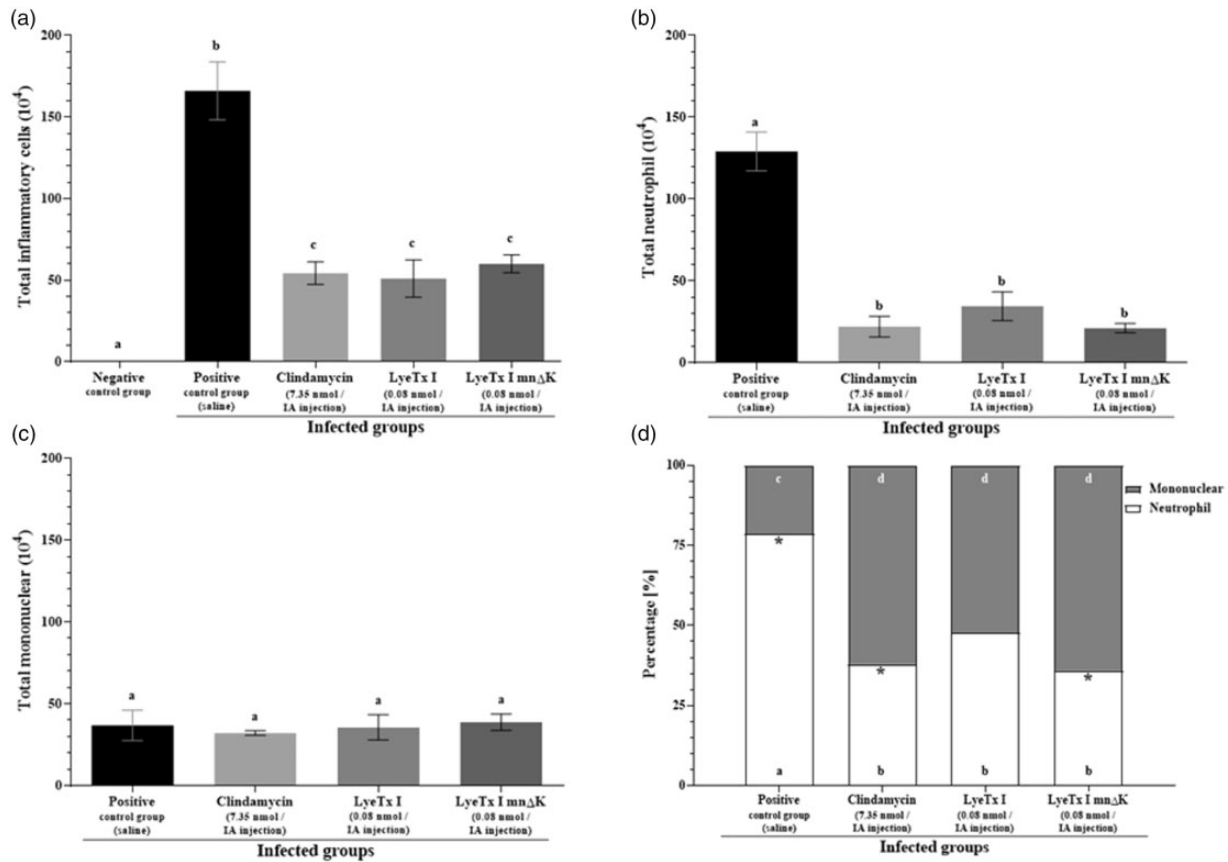
Figure 6. Inflammatory cells recruitment in mice post-treatment. (a) Total cells, (b) total neutrophil, and (c) total mononuclear recruitment per joint cavity. (d) Percentage [%] of neutrophil and mononuclear recruitment per joint cavity. Values are expressed as "mean ± SEM" ($n = 5$). Means of two groups were compared using the Student's t-test. Means of four or five groups were compared using ANOVA, followed by Tukey test for multiple comparisons, two-to-two. Different letters indicate significant differences between groups and asterisks indicate significant difference for the same group ($p < 0.05$).

for positive control group, high total inflammatory cells (Figure 6(a)) and neutrophil recruitments (Figure 6(b)) were observed. However, for treated infected mice, a considerable inflammation reduction was observed compared to positive control group (Figure 6(a) and (b)). Although there was no significant difference in the total mononuclear recruitment between infected groups (Figure 6(c)), the percentage of mononuclear was higher than that of neutrophil for treated infected groups, but not for positive control group (Figure 6(d)). Inflammatory cells recruitment was also investigated in non-infected mice, showing similar results between treated non-infected mice and negative control group. Finally, the removal threshold hypernociception was measured (Figure 7). Data showed that all treated infected groups presented higher values compared to positive control group.

Discussion

The original peptide LyeTx I (control) and three novel shortened derivatives from LyeTx I (LyeTx I mn; LyeTx I mnΔK; LyeTx I mnΔKAc) were synthesized by stepwise solid-phase using the Fmoc strategy. Initially, we have planned to synthesize a shortened derivative from LyeTx I minimized to 15 amino acid residues (LyeTx I mn). However, post-synthesis, a subproduct with a lysine residue included in the fifth position of the amino acid residues
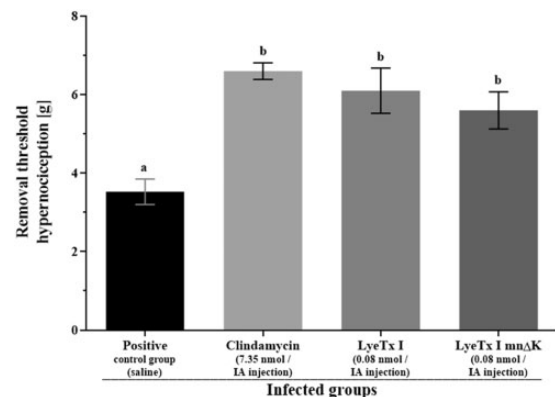

Figure 7. Measurement of the removal threshold hypernociception [g]. Values are expressed as "mean ± SEM" ($n = 4$). Means were compared using ANOVA, followed by Tukey test for multiple comparisons, two-to-two. Different letters indicate significant differences between groups ($p < 0.05$).

sequence (LyeTx I mnΔK) was founded, revealing a theoretical amphipathic structure by *in silico* analysis. Then, this subproduct and its acetylated variation (LyeTx I mnΔKAc) were also synthesized. Crude products were purified by RP-HPLC and the collected fractions were assessed by MALDI-ToF-MS analysis, confirming the achievement of pure products.

CD spectroscopy analysis suggested that the three novel shortened derivatives from LyeTx have a membranolytic activity, similar to the original peptide.[8] They present a random structuring in water and fold as an alpha helix structuring in TFE, suggesting that they probably fold this way in membrane. In SDS, which can be an extrapolation to bacteria membranes (negative net charge), these derivatives folded very well, especially those with the lysine residue included (LyeTx I mnΔK and LyeTx I mnΔKAc). On the other hand, DPC can be an extrapolation to mammalian red cells membrane (neutral net charge) and, in this case, the shortened derivative LyeTx I mnΔK presented the poorest structuring.

In general, both shortened derivatives with the lysine residue included, LyeTx I mnΔK and LyeTx I mnΔKAc, presented higher *in vitro* antimicrobial activities compared to the other shortened derivative, LyeTx I mn. This issue could be explained by the increment in the positive net charge of the molecules produced by the lysine residue inclusion, favoring electrostatic and, then, hydrophobic interactions with microorganism cells.[6,7] Although an *in vitro* antimicrobial activity reduction was observed to the three novel shortened derivatives compared to the original LyeTx I, erythrocyte toxicity assay revealed lower hemolytic activities for these shortened derivatives. These results suggest a poorest interaction between them and mammalian red cells membrane, i.e. highest selectivity for microorganism cells. The hemolytic activity was especially lower for the shortened derivative LyeTx I mnΔK, which displays the highest ratio between geometric average of MIC (antimicrobial activity) and MHC (hemolytic activity) among the three novel shortened derivatives.

Therefore, this derivative (LyeTx I mnΔK) was further assessed by NeuriTox test and compared to the original LyeTx I. Data demonstrated clear differences between both peptides in cytotoxicity on LUHMES cells at different stages of differentiation, regarding to both endpoints: V and NA. The shortened derivative LyeTx I mnΔK was less cytotoxic to LUHMES cells with neurites in development and mature neurites compared to original LyeTx I. During the process of discovering new potential pharmacological compounds, cytotoxicity measures using mammalian cells are indispensable, such as immunotoxicity, cardiotoxicity, hepatotoxicity, nephrotoxicity, and neurotoxicity. Here, we selected the predictive model using LUHMES cells, which is based on neurons and is highly sensitive to hazardous chemicals, allowing specific neurotoxicity evaluation and being used as an important tool to distinguish toxicity among compounds.[18,23] Both cell V and NA of LUHMES cells can be quantitatively evaluated for neurites in different stages of differentiation. Reduction of these parameters after treatment is correlated with compounds toxicity.

Therefore, an overall analysis of our *in vitro* data indicates that the shortened derivative LyeTx I mnΔK is the best candidate to trial as a new antimicrobial agent. Then, it was chosen for further *in vivo* assays and compared to the original LyeTx I.

In vivo antimicrobial activity was evaluated by bacterial recovery assay, which was approximately 10-times lower for those treated infected groups compared to positive control group. It is pertinent to clarify that shortened derivative LyeTx I mnΔK was employed in two doses, 0.08 and 0.16 nmol/IA injection, with no significant difference between them. Thus, only the lower dose (0.08 nmol/IA injection) was further used. Septic arthritis treatment was also evaluated by scintigraphic imaging using 99mTc-CFT, which specifically binds to bacteria, like *S. aureus*.[24] If no bacteria are present, like in negative control group, this radiotracer does not accumulate in the investigated site. On the other hand, there is a positive correlation between bacteria concentration and 99mTc-CFT uptake by infectious site. This is the reason why, for positive control group, scintigraphic imaging showed high 99mTc-CFT uptake by the untreated infected joint. On the other hand, all treated infected groups exhibited 99mTc-CFT uptake similar to that of negative control group. Therefore, both bacterial recovery assay and scintigraphic imaging were in agreement, showing treatment effectiveness for LyeTx I mnΔK.

We also evaluated the inflammatory process reduction post-treatment, by assessing total and differential counts of inflammatory cells. No apparent inflammation was induced by the injection procedure, once no inflammatory cells recruitment was observed for negative control group (sterile PBS inoculation). On the other hand, several immune cell types are associated to the immunological response against *S. aureus* in the articulation. Neutrophils are the first cells to reach infected sites, controlling infection due to their arsenal to fight against pathogens.[25,26] Thus, the higher amount of neutrophils in the joint of positive control mice indicates an intense inflammatory response. On the other hand, for inflammatory process resolution, pathogen elimination, as well as leucocytes and cellular debris reduction, is necessary in order to re-establish tissue homeostasis. Apoptotic polymorphonuclear is phagocytosed by macrophages.[27,28] Then, mononuclear increment in the joints of those treated infected mice suggests inflammatory process reduction. Beyond that, we investigated if treatment by itself produces any inflammation response. In this sense, inflammatory cells recruitment was also investigated in non-infected mice and similar results were observed between treated non-infected mice and negative control group, indicating that treatment induced no apparent inflammation by itself. Thus, the inflammatory process observed in animal's joints was due to the presence of *S. aureus*, and its reduction is related to bacterial decrease post-treatment.

Finally, we evaluated inflammation symptoms reduction. One important clinical feature of septic arthritis is pain, an unpleasant sensory and emotional experience associated with actual or potential tissue damage, involving cognitive, emotional, and structural (nociceptor neurons) aspects.[29,30] Thus, for animals, the most suitable term is nociception or hypernociception.[31] In this sense, we measured the removal threshold hypernociception, which is the maximum pressure in the infected paw tolerated by mice after which animals remove it. All treated infected groups presented higher removal threshold hypernociception compared to positive control group, which is in accordance to previous data, the lower the rate of bacteria and inflammation in the infected joints post-treatment, the

higher the removal threshold hypernociception. Actually, neutrophils are involved in the hypernociception,[32] releasing several hypernociceptive mediators, including prostaglandins, which contribute to a lower removal threshold hypernociception for positive control group.

It is important to emphasize that, although there was no significant difference between treatments, the dosage of shortened derivative LyeTx I mnΔK was about 92-times lower than that of clindamycin, suggesting its high potential as antimicrobial agent. Furthermore, even though shortened derivative LyeTx I mnΔK and original LyeTx I presented similar *in vivo* results, post-IA injections, the former presents a shortened amino acid residues sequence, which reduces time and cost of synthesis, and may contribute for lower side effects and higher *in vivo* stability.[14–16] The latter is due to the decrease or elimination of enzymatic degradation sites and may result in higher amounts of peptide in the infection site if intravenous administration is used, impacting *in vivo* activity. Therefore, the amino acid sequence shortening approach can improve peptide usage as antibiotic. In addition, it could be optimized combining the peptide with polyethylene glycol, as we recently showed with a closely related peptide (LyeTx I-b) that, when pegylated, was much more effective *in vivo* against pneumonia caused by a resistant strain of *A. baumannii*, than non-pegylated peptide (unpublished data). As already suggested, some formulations also seem to decrease immunogenicity[33] and probably to protect peptide against enzymatic degradation, thus increasing its bioavailability, contributing to reach an optimal condition as an antibiotic drug.

Conclusions

Shortened derivatives from peptide LyeTx I were synthesized and CD spectroscopy analysis suggested a membranolytic activity. *In vitro* assays revealed that shortened derivative LyeTx I mnΔK presents the best score between antimicrobial and hemolytic activities, among the shortened derivatives from LyeTx I, and NeuriTox assay demonstrated that it is less toxic than original LyeTx I. *In vivo* data showed that shortened derivative LyeTx I mnΔK was able to reduce *S. aureus* infection in the septic arthritis mouse model, resulting in inflammatory process and pain reductions. Thus, the derivative LyeTx I mnΔK is the best antimicrobial agent candidate among the shortened derivatives from LyeTx I.

AUTHORS' CONTRIBUTIONS

LLF and JTAJ are both co-first authors and participated in the entire research, performing experiments, analyzing data, and writing the manuscript. LLF and JTAJ contributed equally to this paper. DMS, DB, VLSO, and KAGGG performed some experiments and analyzed the respective data. RCC, PLO, PPM, PSC, LMF, EMSF, JD, ML, JMR, FAA, and AMCP designed experiments, analyzed data, and interpreted the results. SOAF, VNC, and MEL conceived the study, analyzed data, interpreted the results, and revised the manuscript. All authors read and approved the final manuscript.

DECLARATION OF CONFLICTING INTERESTS

The author(s) declared no potential conflicts of interest with respect to the research, authorship, and/or publication of this article.

ORCID iDs

Leonardo Lima Fuscaldi https://orcid.org/0000-0001-7864-1324
Vívian Louise Soares de Oliveira https://orcid.org/0000-0002-1798-5171
Johannes Delp https://orcid.org/0000-0003-3224-0677
Jarbas Magalhães Resende https://orcid.org/0000-0001-9827-7312
Flávio Almeida Amaral https://orcid.org/0000-0002-1695-0612

SUPPLEMENTAL MATERIAL

Supplemental material for this article is available online.

REFERENCES

1. Lupetti A, Welling MM, Pauwels EK, Nibbering PH. Radiolabelled antimicrobial peptides for infection detection. *Lancet Infect Dis* 2003;**3**:223–9
2. Malmsten M. Antimicrobial peptides. *Ups J Med Sci* 2014;**119**:199–204
3. Zhang LJ, Gallo RL. Antimicrobial peptides. *Curr Biol* 2016;**26**:R14–9
4. Andersson DI, Hughes D, Kubicek-Sutherland JZ. Mechanisms and consequences of bacterial resistance to antimicrobial peptides. *Drug Resist Updat* 2016;**26**:43–57
5. Kuppusamy R, Willcox M, Black DS, Kumar N. Short cationic peptidomimetic antimicrobials. *Antibiotics* 2019;**8**:44
6. Zasloff M. Antimicrobial peptides of multicellular organisms. *Nature* 2002;**415**:389–95

7. Lupetti A, Nibbering PH, Welling MM, Pauwels EK. Radiopharmaceuticals: new antimicrobial agents. *Trends Biotechnol* 2003;**21**:70–3

8. Santos DM, Verly RM, Piló-Veloso D, de Maria M, de Carvalho MAR, Cisalpino PS, Soares BM, Diniz CG, Farias LM, Moreira DFF, Frézard F, Bemquerer MP, Pimenta AMC, de Lima ME. LyeTx I, a potent antimicrobial peptide from the venom of the spider *Lycosa erythrognatha*. *Amino Acids* 2010;**39**:135–44

9. Consuegra J, de Lima ME, Santos D, Sinisterra RD, Cortés ME. Peptides: β-cyclodextrin inclusion compounds as highly effective antimicrobial and anti-epithelial proliferation agents. *J Periodontol* 2013;**84**:1858–68

10. Cruz Olivo EA, Santos D, de Lima ME, Dos Santos VL, Sinisterra RD, Cortés ME. Antibacterial effect of synthetic peptide LyeTxI and LyeTxI/β-cyclodextrin association compound against planktonic and multispecies biofilms of periodontal pathogens. *J Periodontol* 2017;**88**: e88–e96

11. Fuscaldi LL, dos Santos DM, Pinheiro NGS, Araújo RS, de Barros ALB, Resende JM, Fernandes SOA, de Lima ME, Cardoso VN. Synthesis and antimicrobial evaluation of two peptide LyeTx I derivatives modified with the chelating agent HYNIC for radiolabeling with technetium-99m. *J Venom Anim Toxins Incl Trop Dis* 2016;**22**:16

12. Reis PVM, Boff D, Verly RM, Melo-Braga MN, Cortés ME, Santos DM, Pimenta AMC, Amaral FA, Resende JM, de Lima ME. LyeTxI-b, a synthetic peptide derived from *Lycosa erythrognatha* spider venom, shows potent antibiotic activity *in vitro* and *in vivo*. *Front Microbiol* 2018;**9**:667

13. da Silva CN, da Silva FR, Dourado LFN, dos Reis PVM, Silva RO, da Costa BL, Nunes OS, Amaral FA, dos Santos VL, de Lima ME, Júnior ASC. A new topical eye drop containing LyeTxI-b, a synthetic peptide designed from a *Lycosa erithrognata* venom toxin, was effective to treat resistant bacterial keratitis. *Toxins* 2019;**11**:203

14. Schottelius M, Wester HJ. Molecular imaging targeting peptide receptors. *Methods* 2009;**48**:161–77

15. Wang G, Epand RF, Mishra B, Lushnikova T, Thomas VC, Bayles KW, Epand RM. Decoding the functional roles of cationic side chains of the major antimicrobial region of human cathelicidin LL-37. *Antimicrob Agents Chemother* 2012;**56**:845–56

16. Wang G, Mishra B, Epand RF, Epand RM. High-quality 3D structures shine light on antibacterial, anti-biofilm and antiviral activities of human cathelicidin LL-37 and its fragments. *Biochim Biophys Acta* 2014;**1838**:2160–72

17. Chan W, White P. *Fmoc solid phase peptide synthesis: a practical approach*. Illustrated. reprinted. Oxford: OUP, 2000, 346 pp.

18. de Souza-Fagundes EM, Delp J, Prazeres PHDM, Marques LB, Carmo AML, Stroppa PHF, Glanzmann N, Kisitu J, Szamosvàri D, Böttcher T, Leist M, da Silva AD. Correlation of structural features of novel 1,2,3-triazoles with their neurotoxic and tumoricidal properties. *Chem Biol Interact* 2018;**291**:253–63

19. Stiegler NV, Krug AK, Matt F, Leist M. Assessment of chemical-induced impairment of human neurite outgrowth by multiparametric live cell imaging in high-density cultures. *Toxicol Sci* 2011;**121**:73–87

20. Amaral FA, Boff D, Teixeira MM. In vivo models to study chemokine biology. *Methods Enzymol* 2016;**570**:261–80

21. Diniz SOF, Siqueira CF, Nelson DL, Martin-Comin J, Cardoso VN. Technetium-99m ceftizoxime kit preparation. *Braz Arch Biol Technol* 2005;**48**:89–96

22. Boff D, Oliveira VLS, Queiroz Junior CM, Silva TA, Allegretti M, Verri WA Jr, Proost P, Teixeira MM, Amaral FA. CXCR2 is critical for bacterial control and development of joint damage and pain in *Staphylococcus aureus*-induced septic arthritis in mouse. *Eur J Immunol* 2018;**48**:454–63

23. Delp J, Gutbier S, Klima S, Hoelting L, Pinto-Gil K, Hsieh JH, Aichem M, Klein K, Schreiber F, Tice RR, Pastor M, Behl M, Leist M. A high-throughput approach to identify specific neurotoxicants/developmental toxicants in human neuronal cell function assays. *ALTEX* 2018;**35**:235–53

24. Diniz SOF, Rezende CMF, Serakides R, Ferreira RLB, Ribeiro TG, Martin-Comin J, Cardoso VN. Scintigraphic imaging using technetium-99m-labeled ceftizoxime in an experimental model of acute osteomyelitis in rats. *Nucl Med Commun* 2008;**29**:830–6

25. Mayer-Scholl A, Averhoff P, Zychlinsky A. How do neutrophils and pathogens interact? *Curr Opin Microbiol* 2004;**7**:62–6

26. DeLeo FR, Diep BA, Otto M. Host defense and pathogenesis in *Staphylococcus aureus* infections. *Infect Dis Clin North Am* 2009;**23**:17–34

27. Serhan CN, Chiang N, Van Dyke TE. Resolving inflammation: dual anti-inflammatory and pro-resolution lipid mediators. *Nat Rev Immunol* 2008;**8**:349–61

28. Kennedy AD, DeLeo FR. Neutrophil apoptosis and the resolution of infection. *Immunol Res* 2009;**43**:25–61

29. Krieg AM. A possible cause of joint destruction in septic arthritis. *Arthritis Res* 1999;**1**:3–4

30. Riedel W, Neeck G. Nociception, pain, and antinociception: current concepts. *Z Rheumatol* 2001;**60**:404–15

31. Le Bars D, Gozariu M, Cadden SW. Animal models of nociception. *Pharmacol Rev* 2001;**53**:597–652

32. Cunha TM, Verri WA Jr, Schivo IR, Napimoga MH, Parada CA, Poole S, Teixeira MM, Ferreira SH, Cunha FQ. Crucial role of neutrophils in the development of mechanical inflammatory hypernociception. *J Leukoc Biol* 2008;**83**:824–32

33. Camacho CJ, Katsumata Y, Ascherman DP. Structural and thermodynamic approach to peptide immunogenicity. *PLoS Comput Biol* 2008;**4**: e1000231